ELSEVIER

Simulation of ordered packed beds in chromatography

Mark R. Schure [a,*], Robert S. Maier [b,1], Daniel M. Kroll [c], H. Ted Davis [d]

[a] *Theoretical Separation Science Laboratory, Rohm and Haas Company, 727 Norristown Road, Box 0904, Spring House, PA 19477-0904, USA*
[b] *Army High Performance Computing Research Center, University of Minnesota, 1100 Washington Avenue South, Minneapolis, MN 55415, USA*
[c] *Department of Medicinal Chemistry and Minnesota Supercomputer Institute, University of Minnesota,*
599 Walter Library, 117 Pleasant Street S.E., Minneapolis, MN 55455, USA
[d] *Department of Chemical Engineering and Materials Science, University of Minnesota, Amundson Hall,*
421 Washington Avenue S.E., Minneapolis, MN 55455, USA

Abstract

A computer simulation of chromatographic dispersion in an ordered packed bed of spheres is conducted utilizing a detailed fluid flow profile provided by the Lattice Boltzmann technique. The ordered configurations of simple cubic, body-centered cubic, and face-centered cubic are employed in these simulations. It is found that zone broadening is less for the fcc structure than the sc and bcc structures and less than a random packed bed analyzed in a previous study in the low flow velocity region used for experimental chromatography. The factors which contribute to the performance of the ordered pack beds are analyzed in detail and found to be dependent both on the nearest surface to surface distance and on the distribution of velocities found in the various packing geometries. The pressure drops of the four configurations are compared and contrasted with the pressure drop from monolithic columns.
© 2004 Elsevier B.V. All rights reserved.

Keywords: Computer simulation; Dispersion; Packed beds; Pressure drop; Mathematical modeling

1. Introduction

Liquid chromatography has evolved in the sophistication of column technology. The earliest columns used for liquid chromatography contained large irregular particles. As column technology matured, modern columns were manufactured that contained spherical particles with diameters typically $\leq 5\,\mu m$ and with narrow size distributions. Variations on the packed bed column [1,2] are now commonly found in the liquid chromatography literature. These include monolithic columns [3,4], packed bed liquid chromatography in a microchip [5], micromachined packing structures on a microchip [6], micromachined structures with membrane filters on a microchip [7], and a host of other configurations. With small chip-based formats for chromatography columns being desirable in parallel separation systems utilized for high throughput applications, the maximum column efficiency is most desirable. This is especially important when complex separations in pharmaceutical and biotechnology applications are to be accomplished in a minimum column length and in a minimum amount of time. Although electrochromatography can deliver enhanced efficiencies, as compared to pressure-driven flow, the problems with electrophoresis and retention occurring simultaneously can produce a very complex separation when charged species are present. Therefore we seek alternative means for increasing the chromatographic efficiency of pressure-driven columns.

One possibility is to use templating methods [8,9] found in nanotechnology to build periodic packing structures, i.e. ordered packing materials. This would lend itself to materials that are uniformly porous and reproducible in terms of pressure drop and performance. Recent experiments show this is feasible in short segments [10], although full prototypes may be difficult to construct experimentally. It would therefore be convenient to estimate the efficacy of ordered sphere packing in chromatographic applications prior to undertaking such a task in the laboratory. Using recently introduced computer simulation techniques [11] based on calculating the complete flow field with the Lattice Boltzmann (LB) technique and then simulating the chromatographic dispersion process within this flow field allows such an estimation

---

* Corresponding author. Tel.: +1-215-641-7854;
fax: +1-215-619-1616.
[1] Present Address: United States Army Corps of Engineers, United States Army Engineer Research and Development Center, 3909 Halls Ferry Road, Vicksburg, MS 39180-6199, USA

to be undertaken. We present the results of these simulations here.

Specifically, we will compare the simulation of chromatographic dispersion of ordered sphere packings in the simple cubic (sc), body-centered cubic (bcc), and face-centered cubic (fcc) lattices. These results will be compared with a random sphere packing calculated previously.

2. Background

A number of basic fluid mechanics studies [12–14] have focused on understanding the flow field of ordered packed beds of particles, mostly spheres. Experimental studies on ordered packed beds [15] have found that the effective diffusivity scales with fluid velocity approximately as the velocity squared over a wide range of velocities.

In a packed bed of particles, the reduced or nondimensional velocity, v, also called the Péclet number, is calculated as:

$$v = \frac{\langle v \rangle d}{D} \tag{1}$$

where $\langle v \rangle$ is the average velocity, d is the particle diameter or relevant length scale, and D is the molecular diffusion coefficient of the tracer in the fluid. The effective longitudinal diffusivity, D_L, which is a measure of dispersion commonly used in engineering studies, is related to the chromatographic plate height H as [16]:

$$H = \frac{d\sigma_L^2}{dL} = \frac{2D_L}{\langle v \rangle} = L\frac{\sigma^2}{\bar{t}^2} \tag{2}$$

where σ_L^2 is the length-based variance of the zone distribution in the column, σ^2 is the time-based variance of the zone distribution measured by an ideal external detector, L is the column length and $\bar{t}$ is the zone mean elution time. The number of plates N is given as L/H. If the plate height H is nondimensionalized by dividing by the particle diameter d to give h, the nondimensional plate height, then:

$$\frac{D_L}{D} = \frac{hv}{2} \tag{3}$$

and

$$h = \frac{2}{v} \cdot \frac{D_L}{D} \tag{4}$$

where Eqs. (3) and (4) relate the effective longitudinal diffusivity to the nondimensional plate height.

Theoretical treatments of the effective longitudinal diffusivity in periodic packings [17–19] have focused primarily on two cases. The first and most important case is where the principle axis of the periodic packing is parallel to the flow axis. The second case is where the principle axis is not parallel to the flow axis. For the first case, which is the case studied in this paper, it has been shown [17–19] that the effective longitudinal diffusivity should scale as the velocity

squared, hence the plate height h should scale linearly with v as dictated by Eq. (4). This is very interesting from a chromatographic model perspective as it suggests that the van Deemter model of chromatographic zone broadening:

$$h = A + \frac{B}{v} + Cv \tag{5}$$

where A, B, and C are constants, should be the correct model for dispersion in ordered packing materials. The van Deemter model is often shown to be inadequate in describing experimental zone broadening at higher v where there is a curvature in h versus v data. Since mechanical dispersion is absent in ordered packs [17–19], a mechanical dispersion term should not be present in dispersion models for ordered packing materials. Mechanical dispersion, also known as eddy dispersion, is the broadening mechanism due to the stochastic nature of the velocity distribution which arises from the randomness of the packed bed geometry. The hypothesis regarding whether the van Deemter model is the correct model for the ordered packs will be tested below on simulated chromatographic zones.

Research in the calculation and simulation of ordered packing flow has taken primarily two directions. In a number of publications [20–23] the pressure drop and fluid drag have been examined using LB simulation methods. These studies found that a complex relationship between fluid drag and the orientation of the pack exists, especially at higher Reynolds number. Other studies [24–28] have examined the scaling of dispersion with velocity. In these studies it has been found that the effective longitudinal diffusivity varies approximately as the velocity squared for ordered packs, as predicted earlier by theory. In three cases [26–28] the LB technique was used for the simulation of the ordered pack. None of these studies examined the dispersion in sc, bcc, and fcc geometries at the low Reynolds number flows needed to model chromatography. In general, chromatography is carried out [11] below a Reynolds number of 0.1. Hence, we perform these calculations and look at dispersion in this region in an attempt to understand the chromatographic consequences of ordered packing materials.

3. Simulations

3.1. Algorithms

The LB technique [29–33] is a relatively new method which is capable of accurate calculation of flow fields in the low to moderate Reynolds number region using parallel computers. Parallel computing is essential in porous flow simulations in order to perform the simulation in a reasonable amount of time and to efficiently utilize the large amounts of memory necessary for the fine numerical grid required to achieve accurate simulations. The use of this technique for calculating flow fields useful in chromatography has been previously discussed [11] as have the algorithms
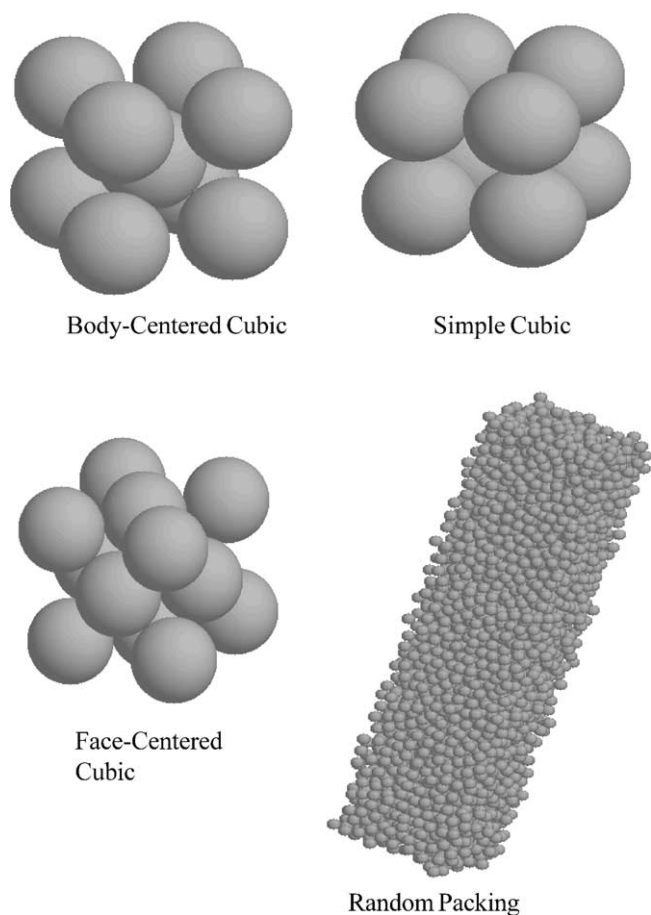
Fig. 1. The four particle packs used in this study.

used to obtain dispersion via a stochastic simulation of convection and diffusion in the flow field [11]. These are used in this paper. As in the previous work, periodic boundary conditions [11] (PBCs) are used in all three dimensions, hence no wall effects are included. The packing material is considered to be internally nonporous. Internal porosity effects can be added after the simulation data is accumulated [11]. The four packing geometries are shown in Fig. 1 for the sc, bcc, fcc, and the random packing geometry analyzed previously.

3.2. Simulation conditions

The simulation conditions are given in Table 1. Velocity rescaling is utilized to cover the whole velocity range for dispersion calculations from one LB simulation per packing

Table 1
The conditions used for simulation

Packing	Grid size (x, y, z)	Porosity
sc	128, 128, 128	0.476
bcc	208, 208, 208	0.320
fcc	256, 256, 256	0.259
Random	256, 256, 1024	0.360

configuration, as described previously [11]. All of the ordered packing flow fields used here were constructed using a Reynolds number of 0.05. The maximum Reynolds number for all of the simulations after rescaling is never over 0.5 for the largest velocity. Hence, inertial effects are absent over the range studied here. All ordered pack particle diameters are 10 μm and all column lengths are 1 cm.

4. Results

4.1. Zone efficiency

The results of simulation for the three ordered packs are shown in Fig. 2 in terms of the nondimensional plate height, h, as a function of the nondimensional velocity used in analytical chromatography. In addition, the results from a previous study [11] utilizing a 4000 sphere random packing are shown for comparison. These results suggest that zone dispersion is minimized in low velocity regions by an fcc pack. A wider velocity region is shown in Fig. 3 including velocities much larger than that found in typical experimental chromatography. Here it is seen that the random pack is more efficient (smaller h) at higher velocities.

Mechanical dispersion is absent in the ordered packs [17–19], as stated previously. At higher velocities where mechanical dispersion becomes more dominant, it is known [16] that the plate height increases less rapidly as compared to the normal velocity range. The random pack zone efficiency does not show as deleterious behavior with increasing velocity as does the ordered packs because the increase in h is limited by the onset of mechanical dispersion. In this regard, mechanical dispersion is useful in limiting the loss of efficiency at higher velocity, however, this higher velocity range is never used in experimental chromatography.
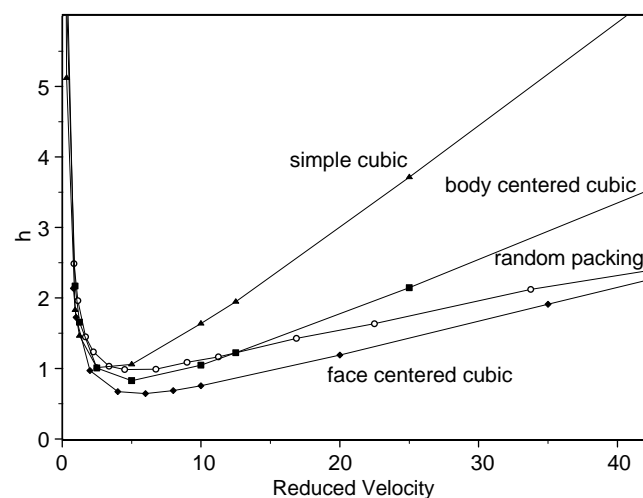

Fig. 2. The dimensionless plate height, h, plotted against the dimensionless average velocity v or Péclet number for the four geometries of particle pack in the lower velocity range up to $v = 40$.
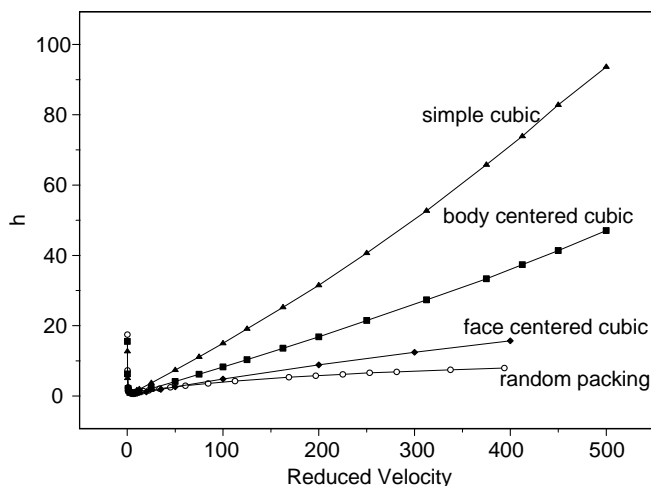
Fig. 3. The dimensionless plate height, h, plotted against the dimensionless average velocity v or Péclet number for the four geometries of particle pack over the full velocity range up to $v = 500$.

4.2. Model fitting

Using nonlinear least-squares analysis, as described previously for the analysis of simulation data [11], a number of models were fit to the ordered pack data. These include the van Deemter model given above in Eq. (5), two variants of the van Deemter model:

$$h = \frac{B}{v} + Cv + Dv^2 \tag{6}$$

and

$$h = \frac{B}{v} + Cv \tag{7}$$

and a variation on the Knox model. The free-exponent Knox model, which was used in the previous simulation paper [11], has the functional form:

$$h = Av^n + \frac{B}{v} + Cv \tag{8}$$

The value of n is usually set to 1/3 but it is allowed to be a free parameter here.

The results of these analyses are shown in Table 2 where the results for $v \le 250$ are separated from the results for $v \le$

Table 2
Percent relative standard deviation (%R.S.D.) of model fits from nonlinear least-squares analysis

Packing	v range	Eq. (5)	Eq. (6)	Eq. (7)	Eq. (8)
sc	$0 \le v \le 250$	17.6	1.50	4.52	4.80
sc	$0 \le v \le 500$	150	2.21	11.2	12.0
bcc	$0 \le v \le 250$	4.64	2.68	1.70	1.73
bcc	$0 \le v \le 500$	45.0	3.33	5.46	5.76
fcc	$0 \le v \le 250$	8.54	4.77	13.8	0.704
fcc	$0 \le v \le 500$	42.7	7.60	20.3	39.3

The models are: Eq. (5), $h = A + B/v + Cv$; Eq. (6), $h = B/v + Cv + Dv^2$; Eq. (7), $h = B/v + Cv$; and Eq. (8), $h = Av^n + B/v + Cv$.

500. As can be seen from this table, the model equations for the ordered packs for $v \le 250$ fit much better much better than the models for the range $v \le 500$. This suggests that the simulation technique, the convection–diffusion mechanics, and/or the models may have inherent differences between these ranges. A number of these aspects are addressed below.

As seen from the results in Table 2, Eq. (5), which includes a velocity-independent term, generally offers the poorest fit to the data over all of the v range. Even Eq. (7), which is the van Deemter equation without the constant term, i.e. a two-parameter model, fits the simulation data better than does the van Deemter model contained in Eq. (5), a three-parameter model. For the bcc data in the lower velocity range (but still far too high for useful experimental separations), the simple two-parameter model of Eq. (7) gives the best fit among all of the models.

The sc and bcc simulation data have a slight positive curvature as v increases in contrast to the fcc simulation data which have a slight negative curvature. Hence, reasonably good fits over the entire range of data are had by the two model equations, Eqs. (6) and (8), which can accommodate curvature at higher v. In the sc and bcc cases, the quadratic model, Eq. (6), fits generally better than does Eq. (8), which contains a variable exponent. One interesting aspect of these curve fits is that the exponent is almost exactly -1.00 for the sc and bcc models when Eq. (8) is used over the full velocity range. One interpretation of this is that the curve fitting is suggesting that the A term in Eq. (8) is not linearly independent of the B term as they become identical when $n = -1$ suggesting that there is no mechanical dispersion present in the data. For the more limited velocity range, the exponent n in Eq. (8) is -1.18 for the fcc simulation data. This suggests that the mostly linear velocity dependence with a slight quadratic behavior can quantitatively explain most of the h versus v data and that the mechanism of zone broadening for these ordered packs is diffusively controlled, as predicted by theory [17–19]. However, the previous theoretical work was not capable of predicting the extent of zone broadening, only its functional dependence, and this is one aspect of why the simulation of these ordered packs is important.

At higher v solute tracers sample the flow field to a lesser extent and the number of plates drops (the plate height increases) because of smaller zone residence times, as indicated by Eq. (2). It is well known [34–36] that zone shape will deviate from nearly Gaussian shape as the number of plates is approximately ≤ 100, although a predominately Gaussian shape is still evident for zones with 25 plates [35]. Since $h = L/Nd$, the simulations will deviate from the results expected for long columns as $h > 10$–20. This may partially explain the curvature at higher velocities exhibited by the simulations.

4.3. Packing geometry

In order to explain the efficiency of the sc, bcc, and fcc results, the normalized pore-size density function, $P(\delta)$, is
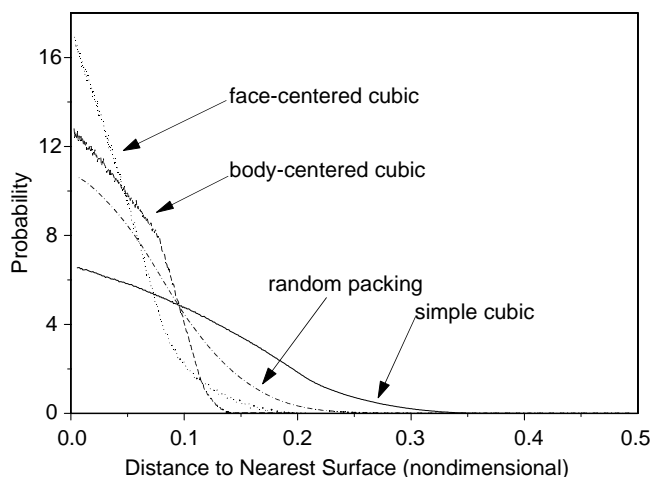
Fig. 4. The surface to surface distance probability density function for the four packing geometries. The independent variable is made nondimensional by dividing by the sphere diameter. The data is filtered with a 10-point moving average window.

calculated and shown in Fig. 4. $P(\delta)\,\mathrm{d}\delta$ is the probability that a random point in the pore space lies at a distance between δ and $\delta + \mathrm{d}\delta$ from the nearest point on the pore-solid interface [37]. In practice, nearest-surface distances are evaluated at each point in a fine three-dimensional lattice superimposed on the pore space, and $P(\delta)$ is compiled from these distances. The average distances and standard deviations are tabulated in Table 3. Normalization is accomplished by dividing the nearest-surface distance by the particle diameter rendering the value dimensionless. For these cases, it is seen that the sc configuration has the widest range of values. The maximum distance value of approximately $1/3$ is obtained within the unit cell and this would lead to zones of higher dispersion than the other configurations. In simple terms, the sc geometry has regions where there are larger distances between particles than the other geometries. This is also reflected in the standard deviation for the sc geometry in Table 3.

The bcc and fcc configurations appear to have similar surface to surface distances as viewed from the results of Table 3 and from the probability densities shown in Fig. 4. This is somewhat surprising as the packing density is higher for fcc than bcc as indicated by the porosity values given in Table 1. As shown in Fig. 4, the fcc surface to surface distance acts over a wider range of values than does the bcc surface to surface distance. Since the chromatographic efficiency varies significantly between the fcc and bcc geometries, some other controlling factor than the surface to

Table 3
The normalized nearest surface distances and standard deviations

Packing	$\bar{d}_N$	σ_N
sc	0.0960	0.0682
bcc	0.0467	0.0307
fcc	0.0417	0.0334
Random	0.0610	0.0459

surface distance must be affecting the zone broadening. Furthermore, the results for the random pack geometry shows that the distance between surfaces probability is higher on average and wider than the bcc configuration yet the random pack performs much better than the bcc pack in terms of efficiency as a function of velocity.

4.4. Velocity analysis

The probability density of flow velocities is given in Fig. 5 for the three ordered packs and the random packing. The fcc flow profile gives a much more uniform probability of finding flow velocities in the region $0 \leq v/\langle v \rangle \leq 1.5$. As a comparison measure, the probability density for the flow velocity in an open cylindrical tube is uniform over all velocities in the range $0 \leq v/\langle v \rangle \leq 1.5$.

Negative velocities are nearly absent from the ordered packs at the velocities of interest. This is a consequence of the creeping flow low Reynolds number hydrodynamics which produces an exceedingly small amount of recirculating flow behind the particles. Substantial recirculation would probably cause broader zones because the flow dynamics would promote a mixing effect.

Negative velocities are somewhat more prevalent in the random pack, but still comprise only a minute fraction of the velocity distribution. In Fig. 5 a small number of negative velocities have been truncated from the random pack probability density. Negative displacements have been observed in real columns, as viewed from NMR-based experiments [38], and these have been interpreted as having a stagnant pool origin in porous particle chromatography. The simulations here have no internal particle porosity, hence, the origin of this for the random packed bed is probably some form of off-axis laminar flow from the random nature of the packing geometry.

As shown in Fig. 5, the bcc and sc velocity probability densities have a wider range than the fcc. In particular, the sc and bcc have higher normalized velocities than the fcc.
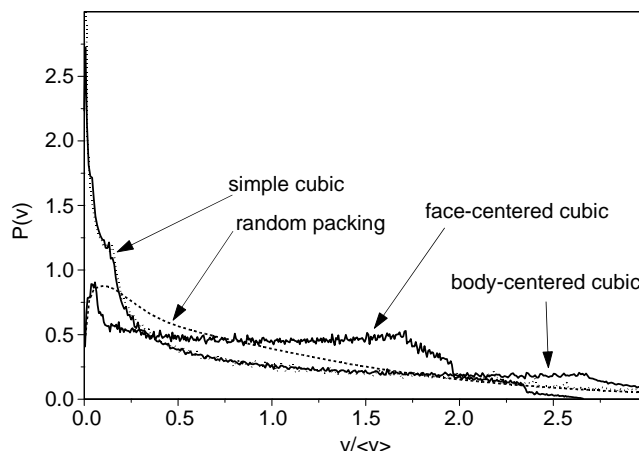

Fig. 5. The flow velocity probability density function for the four packing geometries. The independent variable is made nondimensional by dividing by the average velocity $\langle v \rangle$.

The random packing has a wider range of velocities than the ordered packs, but fewer small velocities than the sc and bcc packings. The velocity probability densities in the low velocity region are inversely related to the efficiencies, with sc > bcc > random pack > fcc. Hence, the efficiency results given in Figs. 2 and 3 can partially be explained by the probability density of the flow velocities given in Fig. 5.

4.5. Pressure drop

The LB technique can compute the pressure drop per unit length, dp/dz, as part of the flow calculation. From the pressure drop, other parameters such as the permeability and the flow resistance are useful in providing a quantitative description of flow in porous media.

The permeability of an isotropic porous medium is a scaler, k, such that [39–41]:

$$q = -\frac{k}{\mu} \cdot \frac{dp}{dz} \tag{9}$$

where q is the superficial velocity [39–41] given by $q = \epsilon \langle v \rangle$, μ is the fluid viscosity, and ϵ is the porosity. Eq. (9) is rearranged to:

$$k = -\frac{\langle v \rangle \mu \epsilon}{dp/dz} \tag{10}$$

noting that the negative sign is present because dp/dz is negative. The permeability, which has units of area, can be nondimensionalized into a flow resistance parameter, ϕ, by [39,40]:

$$\phi = \frac{\epsilon d^2}{k} \tag{11}$$

The values for k and ϕ are given in Table 4 for the three ordered packs and the random pack. The numbers in this table are scaled for a 5 μm sphere diameter where needed and μ is the viscosity of water which is approximately 0.01 P.

The numbers in Table 4 indicate that the permeability is in the order fcc < bcc < random pack < sc for the simulated packs. This is the same order as the porosities given in Table 1 for the simulated packs. For the the flow resistance parameter, ϕ, the order is fcc > bcc > random pack > sc which is the reverse order of the permeability numbers.

These numbers can be contrasted with experimental values from the literature. Typical experimental columns are known [40] to have ϕ values of 500–1000 and the fcc packing

Table 4
The pressure drop, dp/dz for 5 μm spheres, the permeability, and the flow resistance for the three ordered packs and the random pack

Pack	Pressure drop dp/dz (kg/m^2/s^2)	Permeability k (m^2)	Flow resistance ϕ (nondimensional)
sc	7.76×10^7	6.14×10^{-14}	194
bcc	2.58×10^8	1.24×10^{-14}	645
fcc	6.10×10^8	4.25×10^{-15}	1520
Random	2.23×10^7	1.61×10^{-14}	559

clearly is much higher than the bcc and random pack simulations which fall in this range. In an experimental study [42] which included both monolithic and packed bed columns, the value of ϕ for one reversed phase column with 5 μm particles (called Capcellpack C_{18}) was between 555 and 1000 depending on how the permeability was measured. Although the definition of permeability in that study was different than the one used here, the definition of ϕ was identical to Eq. (11), i.e.:

$$\phi = -\frac{d^2}{\mu \langle v \rangle} \cdot \frac{dp}{dz} \tag{12}$$

The experimental results are completely consistent with the simulations noting that the sc configuration gives a very small ϕ value. Monolithic columns in that study [42] with pore size ≈5 μm gave ϕ values between 62 and 95. This suggests that the monolithic columns typically have about one-fifth the flow resistance as do packed columns and that an fcc column would be expected to have about three times the flow resistance as a packed column.

4.6. Separation impedance

Bristow and Knox [43] developed a performance metric which gives the ratio of efficiency to permeability; they termed this nondimensional metric the "separation impedance," E. It is worthwhile to examine this parameter and determine whether the fcc configuration offers better performance than a typical random-packed bed would offer when the increase in pressure drop is included as part of the efficiency measure.

The separation impedance E is defined as [43]:

$$E = \frac{H^2}{k} = h^2 \phi \tag{13}$$

so that high efficiency columns with low pressure drops would tend to have smaller values of E and less efficient columns with higher pressure drops would give higher values of E.

In the case of the fcc pack, $E \approx 550$ when $h_{min} \approx 0.6$ at $\nu \approx 5.0$ as contrasted with the values quoted [42] for the monolithic packings of 300–700 at h_{min}. This is also in contrast to the experimental value of $E \approx 3500$ for the C_{18} column data [42] used in that study. The simulated random packing material data gives $E \approx 1550$ which is less than half that quoted for the experimental values. Again, the simulated pack was constructed at the random packing limit of 36% porosity, which is a tighter pack than that usually found for experimental columns and the efficiency was calculated in the absence of wall effects. In terms of the separation impedance E, the fcc pack is quite good due to the lower h values. Since most applications of the fcc pack would be found in very short columns, for example, in a chip format, the increased flow resistance might not be a problem and the efficiency gain might offset the increased pressure drop. A very recent study [44] examined the flow through an ordered

two-dimensional array of "pillars" (cylinders). It was found that $h_{min} = 0.65$ under specific conditions with E values as small as 200. The chip format was also suggested as a possible method for implementation.

5. Discussion

We have presented results which suggest that an fcc packed assembly of particles can deliver a significant enhancement in lower plate height than a randomly packed bed of particles within the velocity range where h_{min} occurs. This enhancement is predicted in the absence of wall effects. Wall effects would be expected to contribute a fair amount of broadening to an ordered pack, for example, in the chip configuration, where particles would be added in layers to establish the packing in the ordered state. However, embedding the sides of the ordered packs could help alleviate the wall effects, as has been suggested in previous simulations and as implemented in radial compression columns many years ago.

One of the more difficult aspects of making ordered packing materials is to preserve the fcc order. As the results in this paper suggest, bcc defects would tend to reduce the efficiency of the pack. Making an sc pack may be most difficult as the sc pack would tend to collapse to the lower energy fcc structure. But crystal defects probably favor a local bcc structure and this would have to be carefully controlled.

Finally, we note that the simulation of packing materials frees the researcher from the tedious job of making ordered packings to test them. This capability provides a test bed for new materials in separation science and in this respect chromatography has become another area where "computer aided design" principles can be established.

Acknowledgements

References

[1] L.R. Snyder, J.J. Kirkland, Introduction to Modern Liquid Chromatography, Wiley, New York, 1979.
[2] P.R. Brown, R.A. Hartwick (Eds.), High Performance Liquid Chromatography, Wiley, New York, 1989.
[3] E.C. Peters, M. Petro, F. Svec, J.M.J. Fréchet, Anal. Chem. 69 (1997) 3646.
[4] D. Lubda, K. Cabrera, W. Kraas, C. Schaefer, D. Cunningham, LC-GC 19 (2001) 1187.
[5] G. Ocvirk, E. Verpoorte, A. Manz, M. Grasserauer, H.M. Widmer, Anal. Methods Instrum. 2 (1995) 74.
[6] B. He, N. Tait, F. Regnier, Anal. Chem. 70 (1998) 3790.
[7] B. He, L. Tan, F. Regnier, Anal. Chem. 71 (1999) 1464.
[8] O.D. Velev, T.A. Jede, R.F. Lobo, A.M. Lenhoff, Nature 389 (1997) 447.
[9] O.D. Velev, T.A. Jede, R.F. Lobo, A.M. Lenhoff, Chem. Mater. 10 (1998) 3597.
[10] M. Wirth, personal communication.
[11] M.R. Schure, R.S. Maier, D.M. Kroll, H.T. Davis, Anal. Chem. 74 (2002) 6006.
[12] H. Hasimoto, J. Fluid Mech. 5 (1959) 317.
[13] A.S. Sangani, A. Acrivos, J. Multi. Fluid 8 (1982) 343.
[14] A.A. Zick, G.M. Homsy, J. Fluid Mech. 115 (1982) 13.
[15] D.J. Gunn, C. Pryce, Trans. Inst. Chem. Eng. 47 (1969) T341.
[16] S.G. Weber, P.W. Carr, in: P.R. Brown, R.A. Hartwick (Eds.), High Performance Liquid Chromatography, Wiley, New York, 1989.
[17] H. Brenner, Phil. Trans. R. Soc. London A297 (1980) 81.
[18] D.L. Koch, R.G. Cox, H. Brenner, J.F. Brady, J. Fluid Mech. 200 (1989) 173.
[19] H. Brenner, D.A. Edwards, Macrotransport Processes, Butterworth-Heinemann, Boston, 1993.
[20] D.L. Koch, A.J.C. Ladd, J. Fluid Mech. 349 (1997) 31.
[21] R.J. Hill, D.L. Koch, A.J.C. Ladd, J. Fluid Mech. 448 (2001) 213.
[22] R.J. Hill, D.L. Koch, A.J.C. Ladd, J. Fluid Mech. 448 (2001) 243.
[23] R.J. Hill, D.L. Koch, J. Fluid Mech. 453 (2002) 315.
[24] J. Salles, J.-F. Thovert, R. Dellannay, L. Prevors, J.-L. Auriault, P.M. Adler, Phys. Fluids A5 (1993) 2348.
[25] D.A. Edwards, M. Shapiro, H. Brenner, M. Shapira, Transp. Porous Media 6 (1991) 337.
[26] D. Grubert, Int. J. Mod. Phys. C 8 (1997) 817.
[27] H.W. Stockman, R.J. Glass, C. Cooper, H. Rajaram, Int. J. Mod. Phys. C 9 (1998) 1545.
[28] R.S. Maier, D.M. Kroll, R.S. Bernard, S.E. Howington, J.F. Peters, H.T. Davis, Phys. Fluids 12 (2000) 2065.
[29] G.R. McNamara, G. Zanetti, Phys. Rev. Lett. 61 (1988) 2332.
[30] F. Higuera, J. Jimenez, Europhys. Lett. 9 (1989) 663.
[31] S. Succi, R. Benzi, F. Higuera, in: G. Doolen (Ed.), Lattice Gas Methods: Theory, Applications, and Hardware, Elsevier, Amsterdam, 1991, 219 pp.
[32] R.S. Maier, D.M. Kroll, Y.E. Kutsovsky, H.T. Davis, R.S. Bernard, Phys. Fluids 10 (1998) 60.
[33] S. Succi, The Lattice Boltzmann Equation for Fluid Dynamics and Beyond, Oxford University Press, Oxford, 2001.
[34] J.G. Atwood, M.J.E. Golay, J. Chromatogr. 218 (1981) 97.
[35] G. Guiochon, S.G. Shirazi, A.M. Katti, Fundamentals of Preparative and Nonlinear Chromatography, Academic Press, New York, 1994.
[36] A. Fellinger, Data Analysis and Signal Processing in Chromatography, Elsevier, New York, 1998.

[37] S. Torquato, Random Heterogeneous Materials, Springer, New York, 2002.

[38] U. Tallarek, E. Rapp, T. Scheenen, E. Bayer, H. Van As, Anal. Chem. 72 (2000) 2292.

[39] J.C. Giddings, Dynamics of Chromatography, Marcel Dekker, New York, 1965.

[40] J.C. Giddings, Unified Separation Science, Wiley, New York, 1991.

[41] R.S. Maier, D.M. Kroll, H.T. Davis, R.S. Bernard, J. Colloid Interface Sci. 217 (1999) 341.

[42] H. Minakuchi, K. Nakanishi, N. Soga, N. Ishizuka, N. Tanaka, J. Chromatogr. 171 (1998) 121.

[43] P.A. Bristow, J.H. Knox, Chromatographia 10 (1977) 279.

[44] P. Gzil, N. Vervoort, G.V. Baron, G. Desmut, Anal. Chem. 75 (2003) 6244.